# PERFORMANCES OF AUTOMATED CONTROL SYSTEM OF MEMBRANE GAS ABSORPTION: OPTIMIZATION STUDY

*A.R. Sunarti[a] and A.L Ahmad[b]*
*[a]Faculty of Chemical and Natural Resources Engineering, Universiti Malaysia Pahang, 26300 Kuantan, Pahang, Malaysia.*
*[b]School of Chemical Engineering, Engineering Campus, Universiti Sains Malaysia, 14300, Nibong Tebal, Seberang Perai Selatan, Pulau Pinang. Malaysia.*
*Email: [a]sunartirahman@gmail.com , [b] chlatif@usm.my*

**Abstract-** Membrane gas absorption (MGA) can overcome the major drawbacks of the processes that have been used commercially for the removal of $CO_2$. Using produced thin film composite (TFC) membrane, performances of automated control system of MGA was optimized using central composite design (CCD) of Response Surface Methodology (RSM). ANOVA result showed that the temperature, concentration, velocity and flow rate of DEA played a significant role. The optimum DEA temperature was found at 50$^{o}$C, DEA concentration at 2M, velocity at 3770m/s and 80 ml/min of DEA flow rate with 0.90 of desirability.

Keywords: Membrane gas absorption, DEA, RSM

## 1.0 Introduction

Membrane gas absorption (MGA) is a hybrid of membrane and solvent separation that seeks to exploit the advantages of both processes [1,2]. MGA involves the transfer of $CO_2$ through a non-selective membrane before chemically absorption into a liquid absorbent. The polymeric membrane facilitates a controlled flow of gas into the solvent and provides high gas-liquid contact surface area. This physical separation of the liquid and gas flows eliminates foaming and channeling problems that can occur in classical solvent absorption processes.

In MGA, polymer membrane is should from hydrophobic materials. Hydrophobic materials have little or no tendency to adsorb water and water tends to "bead" on their surfaces (i.e discrete droplets). Hydrophobic materials posses low surface tension values and lack active groups in their surface chemistry for formation of "hydrogen- bonds" with water [3]. Table 1 shows the hydrophobic materials and its surface tension. Lower the surface tension shows higher the hydrophobic character of the materials.

Due to the enhanced greenhouse effect, MGA has been considered to be a promising alternative to conventional and potential large scale application technology for the recovery and removal of $CO_2$ [4]. The various factors such as porosity, membrane dimension, liquid viscosity, chemical reaction on mass transfer in membrane [5-7] gave the impact for the MGA performance.

**Table 1** Hydrophobic materials level [3]

| **Chemical Name** | **Surface Tension (dynes/cm)** |
|---|---|
| Polytetrafluoroethylene (Teflon*) | 18 |

| | |
|---|---|
| Polyvinyllidene fluoride (PVDF) | 25 |
| Polypropylene | 29 |
| Polyethylene | 31 |
| Polystyrene | 33 |
| Amylopectin | 35 |
| Polyepichlorohydrin | 35 |
| Amylose | 37 |

To develop a MGA system, the focus is not only on liquid absorption type but improving the characteristic of membrane is also important. Table 2 is shown the MGA system performance with selected several of liquid absorbents.

**Table 2** MGA system performance with selected chemical as liquid absorbents

| **Type of polymer membrane** | **Module** | **Liquid Absorbent** | **Durability** | **Reference** |
|---|---|---|---|---|
| PP[1] | Hollow Fiber | Aqueous NaOH and DEA solution | poor | [8] |
| PP[1] | Celgard X40-200 and X50-215, Hollow Fiber | Aqueous DEA solution | poor | [9] |
| PP[1] | Hollow Fiber | MEA | Wetting after some hours | [10] |
| PES[2] coated with PDMS[3] | Hollow Fiber | MEA | Wetting after 6 hours | [10] |
| PP[1] coated with PDMS[3] | Hollow Fiber | MEA | Wetting after 7 days | [10] |
| PTFE[4] | Hollow Fiber | 5 M MEA | More than 6600 hours | [11] |
| PP[1] | Hollow Fiber | 2M DEA | Over 3 months | [5] |

PP[1]= Polypropylene, PES[2]= Polyether Sulfone, PDMS[3]= polydimethylsiloxane (silicon rubber), PTFE[4]= Polytetrafluoroethylene

Commercial MGA system are available on the market, however they tend to produce mass transfer coefficients that are significantly lower than those obtained in modules that are carefully

built by hand [12]. The poor performance of commercial modules had been attributed to an uneven spacing of flat sheet membrane within the system, resulting in liquid channeling [13]. Furthermore, the experimental analysis of commercial modules is limited because they only have data sampling ports at the inlets and outlets. Hence, in this study, an automated control system of MGA was designed and fabricated in-house for the purpose to enhance the membrane performances. Performances of MGA were investigated based on selected operating parameters. A CCD and RSM were used to identify the significant operating parameters and developed a model to predict the response of the mass transfer rate of $CO_2$.

## 2.0 Methods/Theory

### 2.1 *Materials*

Thin film composite (TFC) membranes were used. A 99% grade of diethanolamines (DEA) were purchased from Merck (M) Sdn. Bhd. and were mixed with deionized water, respectively to prepare aqueous liquid absorbents with desired concentrations (1M, 2M and 3M). The properties of TFC membranes are listed in Table 3.

**Table 3** Properties of TFC membrane

| **Properties** | |
|---|---|
| TFC membrane type | PDMS based 0.1 μm PVDF membrane |
| Contact angle with water | $130.2^o$ |
| Contact angle with 1M of DEA | $144.2^o$ |
| Contact angle with 2M of DEA | $138.1^o$ |
| Contact angle with 3M of DEA | $131.4^o$ |

### 2.2 *Design of automated control system of MGA*

In this study, an automated control system of MGA was designed and fabricated in-house. The schematic diagram for experimental setup is listed in Table 4 together part of shown in Figure 1.

**Table 4** Part of list

| **Part Number** | **Description** |
|---|---|
| 1 | Frame |
| 4 | Stainless steel membrane cell |
| 6 | Hot water tank for temperature controller |
| 8 | Pump for hot water circulation |
| 9 | $CO_2$ gas sensor |
| 11 | Control panel |

| | |
|---|---|
| 12 | Gas tank to supply $CO_2$ and $N_2$ |
| 15 | Feed tank for supply liquid absorbent |
| 18 | Dosing pump as chemical resistant pump |
| 23 | Product tank |

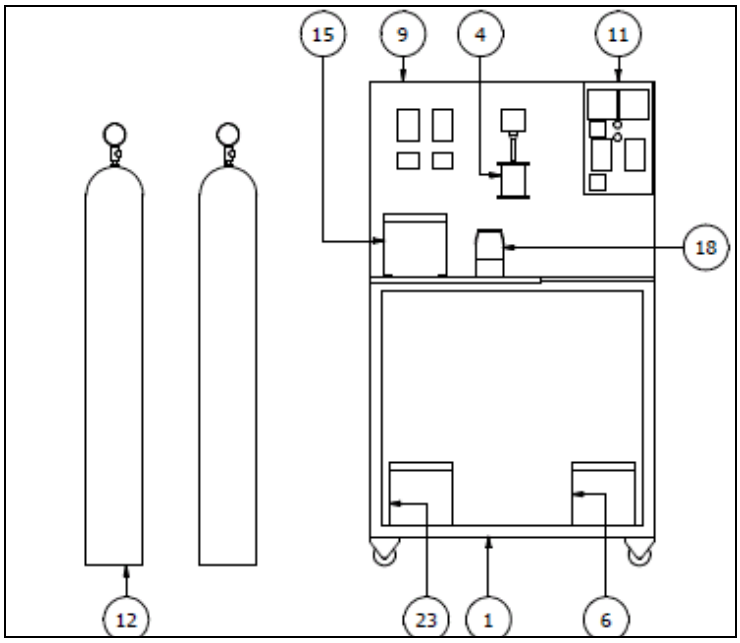


**Figure 1** Schematic diagram for automated control system of MGA

The gas stream was passed through the upside of membrane cell and diffused through membrane pores into the liquid absorbent. Here, supply pressure regulator was ranged 0 to 5 bars applied. Gas flow meters with digital display were applied which ranged 0 to 400 ml/min. To detect $CO_2$ flow, $CO_2$ composition sensors was located before and after membrane cell for determine the composition of $CO_2$ which ranged 0- 20%. Two units of bourdon type pressure gauges were attached to detect the $CO_2$ and $N_2$ at inlet which ranged 0 to 5 bars. 10 liters hot water bath with centrifugal circulating pump and digital temperature controller (30-70$^oC$) was used to heat up the liquid absorbent. Rotameter was used to feed liquid absorbents. Three liters stainless steel tank was provided as feed tank with liquid feed pump. Electrical control consoled with indicator lamps, safety circuit and emergency cut out switch was allocated at control panel.

Before each run of an experiment, the system was cleaned for at least 10 min by deionized water to eliminate the influence of the former experiment. And all data were obtained at steady state, after at least 30 min of operating time. When $CO_2/N_2$ mixture was used as the feed gas, Gas Chromatography (Perkin Elmer, TCD) was used to analyze the inlet and outlet gases concentrations. The $CO_2$ concentration of the outlet liquid was measured by a $CO_2$ electrode (Thermo Orion Model 95-02) to verify the mass balance via the gas analysis. The measurement range of the electrode was 4.4–440 ppm $CO_2$ with a reproducibility of ±2%. All the data were

collected after experiment had been operated for 10 min to ensure the system to reach the steady state. Steady state was indicated by a constant $CO_2$ concentration in the outlet gas stream. The results of each run were averaged from five times of sampling.

### **2.3** *Calculation of experimental data*

For chemical absorption, the overall mass transfer coefficient was experimentally calculated by following [14]:

$$K_i = \frac{V_g (C_{i,g,in} - C_{i,g,out})}{A_m (\Delta C_m)} \tag{1}$$

where $V_g$ is the volumetric flow rate of gas phase, $A_m$ is the area of the membrane and $\Delta C_m$ is the logarithmic mean driving force based on gas phase concentration:

$$\Delta C_m = \frac{(C_{i,g,in} - C^*_{g,in}) - (C_{i,g,out} - C^*_{g,out})}{\ln[(C_{i,g,in} - C^*_{g,in})/(C_{i,g,out} - C^*_{g,out})]} \tag{2}$$

where $C^*_{g,out}$ and $C^*_{g,in}$ in gas phase concentrations in equilibrium with corresponding liquid-phase $CO_2$ concentrations $C_{i,L}$. Due to liquid –phase $CO_2$ concentrations at inlet of the module equal to 0, $C^*_{g,out}$ is 0. $C^*_{g,in}$ is expressed by Henry's law as: $C^*_{g,in} = C_{i,L}/m$, the value of $m$ is estimated by literature [15].

### **2.4** *Experimental design*

The $CO_2$ mass transfer optimization was studied with a standard Response Surface Methodology (RSM) using central composite design (CCD). CCD was used to examine the relationship between one or more response variables and set of quantitative experimental factors and finally necessary to find the factor settings that optimize the response. It was used to fit a quadratic surface as well. This method helps to optimize the individual and interaction effects of operating parameters of MGA system and its potential of $CO_2$ removal on DEA as liquid absorbent.

In this study, a half-fraction central composite face centered design with single replicate at each point was used to optimize the MGA system. Six variables were investigated in this study, they are coded as; liquid absorbent temperature (30 to 50$^o$C) (**A**), liquid absorbent concentration (1 to 3M) (**B**), liquid absorbents velocity (943 to 3770 cm/min) (**C**), gas flow rate (50 to 120 ml/min) (**D**), liquid absorbents flow rate (25 to 80 ml/min) (**E**), and volumetric concentration of $CO_2$ in inlet (10 to 100%) (**F**). Meanwhile, $CO_2$ mass transfer (mol/ ($m^2$ s)) (**Y**) was analyzed as response. The experimental conditions for each system studied as shown in Table 5.

**Table 5** Variables and levels for two-level fractional study of MGA system

| Symbol | Variables | Range | |
|---|---|---|---|
| **A** | Liquid absorbent temperature | 30 | 50 |
| **B** | Liquid absorbent concentration | 1 | 3 |
| **C** | Liquid absorbents velocity | 943 | 3770 |
| **D** | Gas flow rate | 50 | 120 |
| **E** | Liquid absorbents flow rate | 25 | 80 |
| **F** | Volumetric concentration of $CO_2$ in inlet | 10 | 100 |

The variables which are identified as important or significant are then investigated more thoroughly in subsequent experiment. The CCD consisting of 6 center points and 14 axial points that rendered a total of 46 run of experiment, which used to analyze the data acquired from the experimental design, as shown in Table 6. All experiments were done in a randomized order to minimize the effect of unexplainable variability in the observed responses due to irrelevant factor. Design expert software version 6.0.6 [16] was used to develop the mathematical model and evaluate the subsequent regression analyses, analyses of variance (ANOVA) and response surfaces. Based on the optimum operating parameters calculated by CCD, the optimum condition was repeated and validated.

**Table 6** Design layout and experimental variables for CCD

| Run | Factor A | Factor B | Factor C | Factor D | Factor E | Factor F |
|---|---|---|---|---|---|---|
| 1 | 40 | 2 | 2356.5 | 85 | 52.5 | 100 |
| 2 | 30 | 3 | 943.0 | 120 | 80.0 | 100 |
| 3 | 50 | 1 | 943.0 | 120 | 25.0 | 10 |
| 4 | 40 | 2 | 2356.5 | 85 | 52.5 | 55 |
| 5 | 40 | 2 | 2356.5 | 120 | 52.5 | 55 |
| 6 | 30 | 2 | 2356.5 | 85 | 52.5 | 55 |
| 7 | 30 | 1 | 3770.0 | 120 | 80.0 | 100 |
| 8 | 30 | 3 | 943.0 | 120 | 25.0 | 10 |
| 9 | 50 | 2 | 2356.5 | 85 | 52.5 | 55 |
| 10 | 50 | 3 | 943.0 | 120 | 80.0 | 10 |
| 11 | 30 | 1 | 943.0 | 120 | 80.0 | 10 |
| 12 | 30 | 1 | 943.0 | 50 | 80.0 | 100 |
| 13 | 40 | 1 | 2356.5 | 85 | 52.5 | 55 |
| 14 | 30 | 3 | 943.0 | 50 | 80.0 | 10 |
| 15 | 50 | 3 | 3770.0 | 50 | 25.0 | 100 |
| 16 | 30 | 1 | 3770.0 | 120 | 25.0 | 10 |
| 17 | 50 | 1 | 3770.0 | 120 | 25.0 | 100 |
| 18 | 50 | 3 | 3770.0 | 50 | 80.0 | 10 |
| 19 | 40 | 2 | 2356.5 | 85 | 52.5 | 55 |
| 20 | 30 | 1 | 943.0 | 50 | 25.0 | 10 |
| 21 | 40 | 2 | 2356.5 | 85 | 52.5 | 10 |
| 22 | 50 | 1 | 3770.0 | 120 | 80.0 | 10 |
| 23 | 30 | 3 | 3770.0 | 50 | 80.0 | 100 |
| 24 | 30 | 3 | 3770.0 | 120 | 25.0 | 100 |

| | | | | | | |
|---|---|---|---|---|---|---|
| 25 | 50 | 3 | 943.0 | 50 | 25.0 | 10 |
| 26 | 50 | 1 | 943.0 | 50 | 25.0 | 100 |
| 27 | 50 | 3 | 943.0 | 50 | 80.0 | 100 |
| 28 | 50 | 3 | 3770.0 | 120 | 80.0 | 100 |
| 29 | 40 | 3 | 2356.5 | 85 | 52.5 | 55 |
| 30 | 30 | 1 | 3770.0 | 50 | 80.0 | 10 |
| 31 | 40 | 2 | 2356.5 | 85 | 80.0 | 55 |
| 32 | 50 | 3 | 943.0 | 120 | 25.0 | 100 |
| 33 | 50 | 1 | 3770.0 | 50 | 25.0 | 10 |
| 34 | 50 | 1 | 943.0 | 120 | 80.0 | 100 |
| 35 | 30 | 1 | 3770.0 | 50 | 25.0 | 100 |
| 36 | 40 | 2 | 2356.5 | 85 | 25.0 | 55 |
| 37 | 30 | 3 | 3770.0 | 50 | 25.0 | 10 |
| 38 | 40 | 2 | 943.0 | 85 | 52.5 | 55 |
| 39 | 40 | 2 | 2356.5 | 50 | 52.5 | 55 |
| 40 | 30 | 3 | 3770.0 | 120 | 80.0 | 10 |
| 41 | 50 | 1 | 943.0 | 50 | 80.0 | 10 |
| 42 | 30 | 3 | 943.0 | 50 | 25.0 | 100 |
| 43 | 40 | 2 | 3770.0 | 85 | 52.5 | 55 |
| 44 | 30 | 1 | 943.0 | 120 | 25.0 | 100 |
| 45 | 50 | 1 | 3770.0 | 50 | 80.0 | 100 |
| 46 | 50 | 3 | 3770.0 | 120 | 25.0 | 10 |

## 3.0 Results and discussion

### 3.1 *Response Surface Analysis for DEA as liquid absorbent*

Responses for each experimental run and predicted value are as shown in Table 7.

**Table 7** Experimental and response results

| **Standard order** | **$CO_2$ mass transfer (mol/($m^2$s))** | |
|---|---|---|
| | Experimental values | Predicted values |
| 1 | 0.00140 | 0.00158 |
| 2 | 0.00410 | 0.00416 |
| 3 | 0.00180 | 0.00278 |
| 4 | 0.00220 | 0.00309 |
| 5 | 0.00270 | 0.00241 |
| 6 | 0.00490 | 0.00325 |
| 7 | 0.00170 | 0.00167 |
| 8 | 0.00460 | 0.00428 |
| 9 | 0.00120 | 0.00132 |
| 10 | 0.00310 | 0.00303 |
| 11 | 0.00220 | 0.00230 |

| | | |
|---|---|---|
| 12 | 0.00480 | 0.00503 |
| 13 | 0.00120 | 0.00086 |
| 14 | 0.00310 | 0.00357 |
| 15 | 0.00280 | 0.00304 |
| 16 | 0.00460 | 0.00422 |
| 17 | 0.00230 | 0.00241 |
| 18 | 0.00280 | 0.00325 |
| 19 | 0.00220 | 0.00167 |
| 20 | 0.00470 | 0.00428 |
| 21 | 0.00140 | 0.00158 |
| 22 | 0.00310 | 0.00416 |
| 23 | 0.00280 | 0.00278 |
| 24 | 0.00310 | 0.00309 |
| 25 | 0.00050 | 0.00086 |
| 26 | 0.00420 | 0.00357 |
| 27 | 0.00280 | 0.00304 |
| 28 | 0.00440 | 0.00422 |
| 29 | 0.00140 | 0.00132 |
| 30 | 0.00300 | 0.00303 |
| 31 | 0.00260 | 0.00230 |
| 32 | 0.00470 | 0.00503 |
| 33 | 0.00410 | 0.00585 |
| 34 | 0.00830 | 0.00668 |
| 35 | 0.00290 | 0.00199 |
| 36 | 0.00370 | 0.00383 |
| 37 | 0.00510 | 0.00588 |
| 38 | 0.00680 | 0.00666 |
| 39 | 0.00620 | 0.00627 |
| 40 | 0.00650 | 0.00627 |
| 41 | 0.00670 | 0.00626 |
| 42 | 0.00620 | 0.00628 |
| 43 | 0.00610 | 0.00627 |
| 44 | 0.00620 | 0.00627 |
| 45 | 0.00640 | 0.00627 |
| 46 | 0.00660 | 0.00627 |

The regression model equation generated for the $CO_2$ mass transfer by discarding the insignificant effects which was obtained after performing 46 experiments, are listed in Table 7. The mathematical models were also inspected for its validity by comparing the experimental data and the predicted data given by the models. The data can be observed also in Table 7. This data can be observed using visual inspection by plotting the experimental data versus the predicted data corresponding to the respective responses in the DOE software. The results demonstrated that there are tendencies in the linear regression fit, and the model explained the experimental range studied adequately. The fitted regression equation showed good fit of the models and was successful in capturing the correlation between the variables. From all these validity tests, the

model was found to be adequate for predicting the optimized $CO_2$ mass transfer for MGA system using DEA as liquid absorbent.

### 3.2 *ANOVA analysis*

Apart from that, significant effects of regression model generated for the $CO_2$ mass transfer were tabulated in Table 8. The significant effects included the DEA temperature (*A*), DEA concentration (*B*), DEA velocity (*C*), DEA flow rate (*E*), second-order effects of DEA concentration ($B^2$), as well interaction effect of (*AB*), (*AC*), (*AE*), (*BC*), (*BE*) and (*CE*). The regression model equations were evaluated by F-test ANOVA which revealed that these regressions model equation are statistically significant at 95% confidence level. All these significant effects had the value of Prob > *F* less than 0.05. A quadratic empirical model for $CO_2$ mass transfer is as shown in Equation 3.

**Table 8** ANOVA and variance analysis for $CO_2$ mass transfer model

| **Response** | | **Sum of Squares (SS)** | **Mean Square (MS)** | **F- Value** | **Prob > F** | **Remark** |
|---|---|---|---|---|---|---|
| Quadratic Model | | $1.44 \times 10^4$ | $1.31 \times 10^5$ | 28.62 | < 0.0001 | Significant |
| | A | $5.76 \times 10^6$ | $5.76 \times 10^6$ | 12.59 | 0.0012 | Significant |
| | B | $2.86 \times 10^5$ | $2.86 \times 10^5$ | 62.53 | < 0.0001 | Significant |
| | C | $5.20 \times 10^6$ | $5.20 \times 10^6$ | 11.36 | 0.0019 | Significant |
| | E | $2.65 \times 10^9$ | $2.65 \times 10^9$ | $5.78 \times 10^3$ | 0.0093 | Significant |
| | $B^2$ | $9.98 \times 10^5$ | $9.98 \times 10^5$ | 218.03 | < 0.0001 | Significant |
| | AB | $1.13 \times 10^8$ | $1.13 \times 10^8$ | 0.025 | 0.0087 | Significant |
| | AC | $1.51 \times 10^7$ | $1.51 \times 10^7$ | 0.33 | 0.0056 | Significant |
| | AE | $2.81 \times 10^7$ | $2.81 \times 10^7$ | 0.61 | 0.0438 | Significant |
| | BC | $1.25 \times 10^7$ | $1.25 \times 10^7$ | 0.27 | 0.0060 | Significant |
| | BE | $5.00 \times 10^7$ | $5.00 \times 10^7$ | 1.09 | 0.0030 | Significant |
| | CE | $3.64 \times 10^5$ | $3.64 \times 10^5$ | 7.96 | 0.0079 | Significant |
| Lack of Fit | | $1.56 \times 10^5$ | $4.71 \times 10^7$ | 23.56 | 0.1620 | Not Significant |

Model of $CO_2$ mass transfer:

$$Y = 6.267E\text{-}003 + 4.118E\text{-}004\ (A) + 9.176E\text{-}004\ (B) + 3.912E\text{-}004\ (C) + 8.824E\text{-}006\ (E) - 3.355E\text{-}003\ (B^2) + 1.875E\text{-}005\ (AB) + 6.875E\text{-}005(AC) - 9.375E\text{-}005\ (AE) - 6.250E\text{-}005\ (BC) + 1.250E\text{-}004\ (BE) + 3.375E\text{-}004\ (CE) \quad (3)$$

In this study, the reggression model of $CO_2$ mass transfer (Equation 3) provided high values of $R^2$ (0.9025), Adj-$R^2$ (0.8710) and Pred- $R^2$ (0.8277) as shown by Table 9. The high determination coefficient of $R^2$ indicated that the variability in the response could be explained by the mathematical model. For the model of equation, the predicted $R^2$ is in reasonable agreement with the adjusted $R^2$ because they are within 0.10 to each other.

**Table 9** Summary of ANOVA and regression analysis for $CO_2$ mass transfer

| Model | Significant Model Terms | Standard Deviation | $R^2$ | Adj-$R^2$ | Pred-$R^2$ | Adequate Precision |
|---|---|---|---|---|---|---|
| Quadratic Model | A,B,C,E,$B^2$, AB,AC, AE, BE, CE | 6.767 x $10^{-3}$ | 0.9025 | 0.8710 | 0.8277 | 16.846 |

### 3.3 *Analysis of response surface*

Impacts of DEA temperature, DEA concentration, DEA velocity and liquid absorbent flow rate were significant as indicated by response surface plot in Figure 2 to Figure 7. The maximum mass transfer of $CO_2$ was attained at intermediate DEA concentration (1M to 3M) in Figure 2, Figure 3 and Figure 4, respectively.

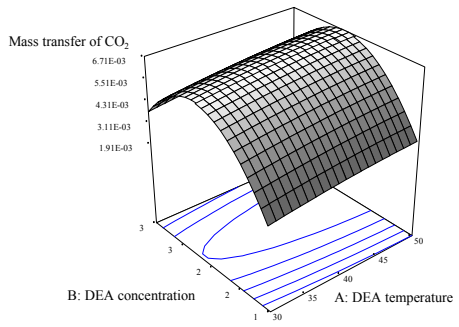


**Figure 2** Response surface plotted on DEA concentration: DEA temperature

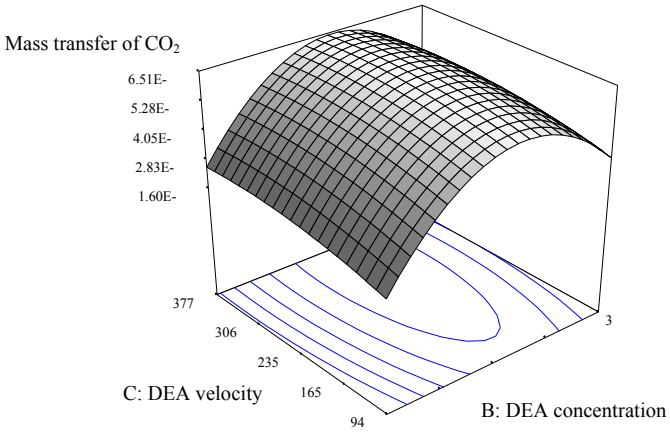


**Figure 3** Response surface plotted on DEA concentration: DEA velocity

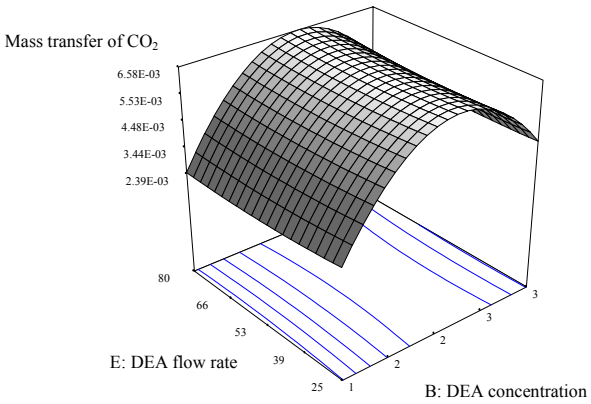


**Figure 4** Response surface plotted on DEA concentration: DEA flow rate

At DEA concentration of less than 2M, the effects of elongation contributed to greater mass transfer of $CO_2$, as shown in Figure 2. However, at DEA concentration more 2M, the elongation gave minor effect on the mass transfer of $CO_2$ where an almost straight line was observed on the contour plot in Figure 2. This could be due to the DEA was consumed with continuous supplied of $CO_2$. However, increased in the DEA temperature resulting in drop in DEA concentration, which was lead to drop in $CO_2$ mass. Hence, the MGA system still needed to be run under appropriate level of DEA concentration and DEA temperature; so that the $CO_2$ mass transfer would be in good performance.

On the other hand, in Figure 3, higher mass transfer of $CO_2$ was noted when the fast DEA velocity and intermediate of DEA concentration were introduced during the MGA system operated. In Figure 4, a similar trend was observed, where intermediate DEA concentration and the fast DEA flow rate were necessary for maximum mass transfer of $CO_2$.

Referring to the three- dimensional surface counter plots in Figure 5, mass transfer of $CO_2$ was found lower when DEA run under low temperature and high elongation. The maximum of $CO_2$ mass transfer was found at 5.96 x $10^{-3}$ mol/$m^2$s when the DEA temperature was 30$^o$C and 2357 m/s of DEA velocity.

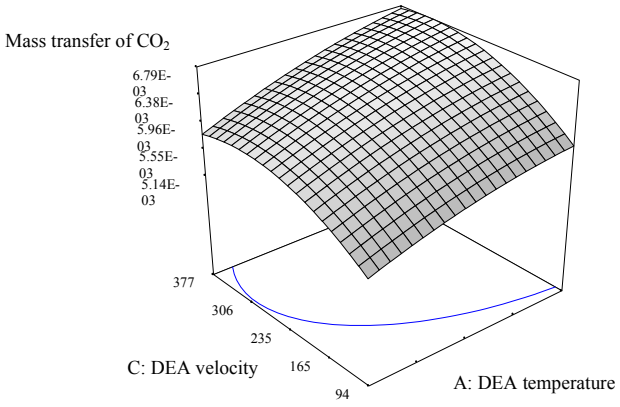


**Figure 5** Response surface plotted on DEA velocity: DEA temperature

Impacts of DEA flow rate, DEA velocity and DEA temperature were shown in Figure 6 and 7. At higher DEA flow rate, the MGA system still needed higher DEA velocity and DEA temperature, where long elongation as can be seen in Figure 6 and 7. Hence, at 80 ml/min of DEA flow rate and 943 m/s of DEA velocity, $CO_2$ mass transfer was found at 4.93 x $10^{-3}$ mol/$m^2$s. Meanwhile, at 80 ml/min of DEA flow rate and 30$^o$C of DEA temperature, $CO_2$ mass transfer was found at 5.61 x $10^{-3}$ mol/$m^2$s. Thus, it can be concluded that $CO_2$ mass transfer depends appropriate value of DEA temperature, velocity and flow rate.

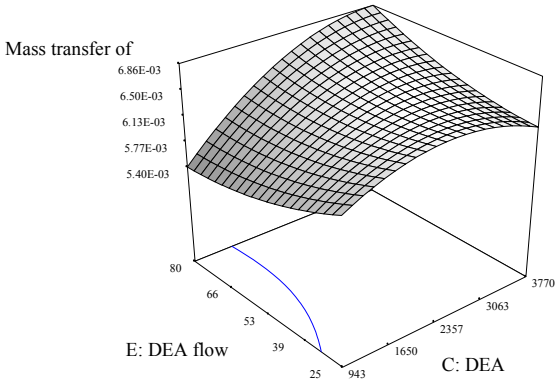

**Figure 6** Response surface plotted on DEA flow rate: DEA velocity

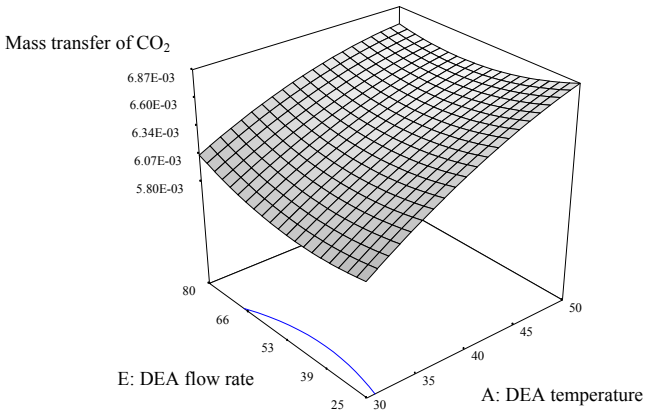


**Figure 7** Response surface plotted on DEA flow rate: DEA temperature

### 3.4 *Verification and statistical models and diagnostic statistic*

RSM has the advantages of observing the interaction effects among independent parameters. Figure 8 to Figure 13 show the binary interactions between DEA concentration and DEA temperature (Figure 8); DEA temperature and DEA velocity (Figure 9); DEA temperature and DEA flow rate (Figure 10); DEA flow rate and DEA velocity (Figure 11); DEA concentration and DEA velocity (Figure 12) and DEA concentration and DEA flow rate (Figure 13), respectively.

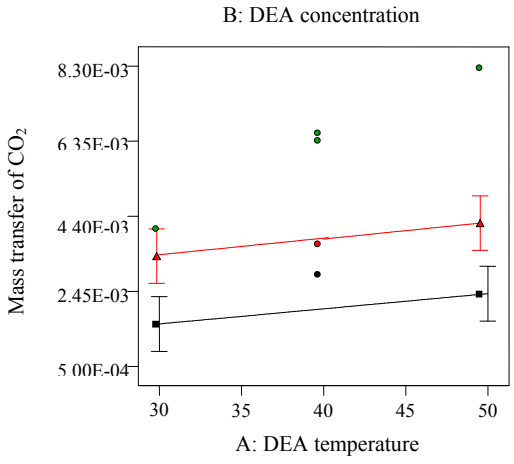


**Figure 8** Interaction via DEA temperature: DEA concentration (▲for 1M, ■ for 3M and ● is design point)

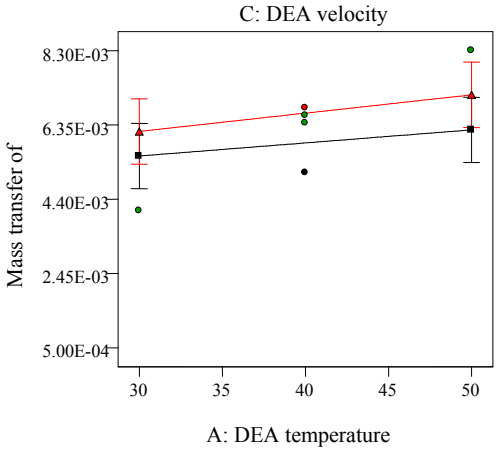


**Figure 9** Interaction via DEA temperature: DEA velocity (▲for 3770 m/s, ■ for 943 m/s and ● is design point)

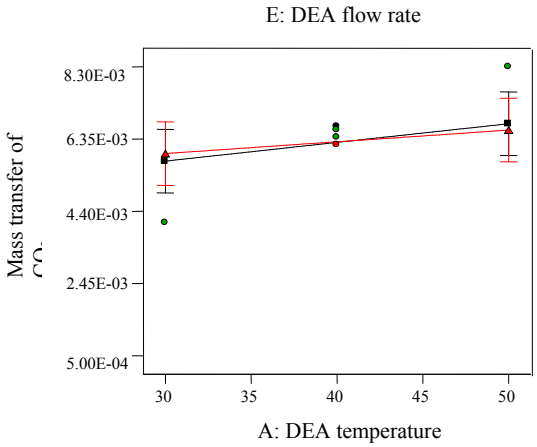


**Figure 10** Interaction via DEA temperature: DEA flow rate (▲for 80 ml/min, ■ for 25 ml/min and ● is design point)

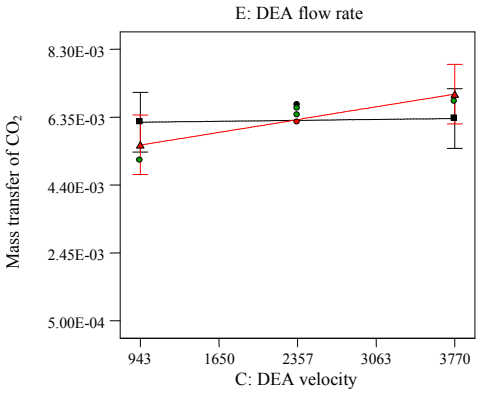

**Figure 11** Interaction via DEA velocity: DEA flow rate (▲for 80 ml/min, ■ for 25 ml/min and ● is design point)

As can be seen in Figure 8 to Figure 11, the parallel curvatures implied that there was a weak interaction between variables. However, the non- parallel curvatures of Figure 12 and Figure 13 indicated that there was relatively strong interaction between variables. In this case, DEA concentration (B), DEA velocity (C) and DEA flow rate (E). As the result of this strong interaction, BC and BE appeared as significant terms in Equation 3. According the model, the maximum operating condition of MGA system was predicted around the region of middle of the variables.

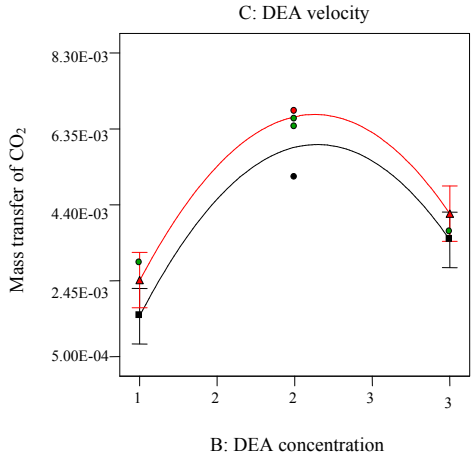


**Figure 12** Interaction via DEA concentration: DEA flow rate (▲for 3770 m/s, ■ for 943 m/s and ● is design point)

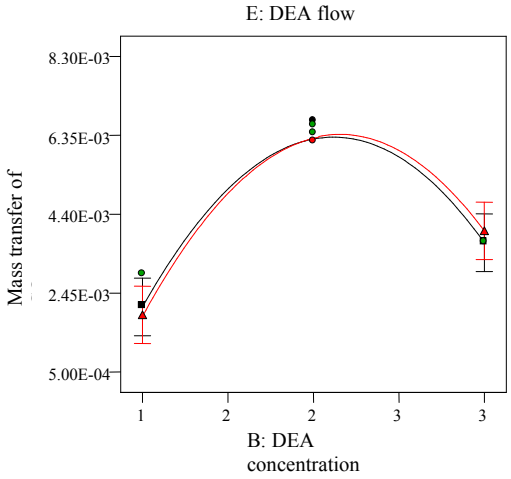


**Figure 13** Interaction via DEA concentration: DEA flow rate (▲for 80 ml/min, ■ for 25 ml/min and ● is design point)

Diagnostic plots in Figure 14 and Figure 15 were used to determine the residual analysis of response surface design, ensuring that the statistical assumptions fit to analysis data. Figure 14 shows the normal probability of the residuals, to verify whether the standard deviations between actual and predicted response values do follow the normal distribution [17]. The general impression from the figure explained that underlying errors were distributed normally as the residuals fall near to a straight line and thus there was no sever indication of non-normality of the experimental results.

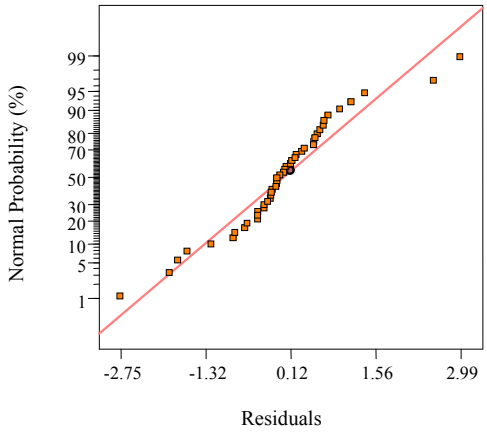


**Figure 14** Normal probability plot of residual for mass transfer of $CO_2$

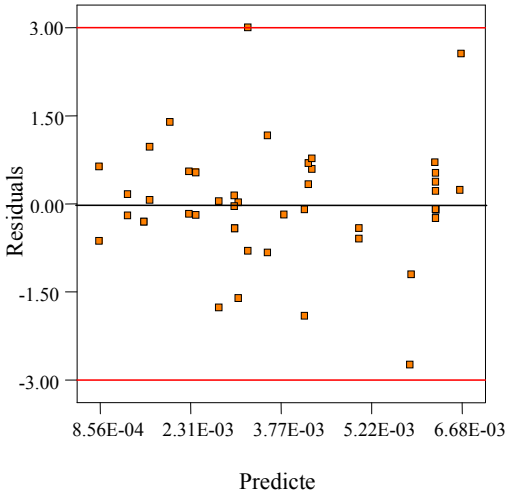


**Figure 15** Plot of residual versus predicted response

The plots of residuals versus predicted response was presented in Figure 15. All points of experimental runs were scattered randomly within constant range of residuals across the graph

i.e. within the horizontal lines at point ±3.0. This implied that the proposed models were adequate and the assumption of constant variance was confirmed.

Reliability and adequacy of empirical models (Equation 3) were confirmed when the actual values obtained from experimental studies were well-matched to the estimated values from regression model (Figure 16). Points above the diagonal line were those over-estimates and vice versa. Figure 16 generally indicated that all experiment design points were distributed along the diagonal line.

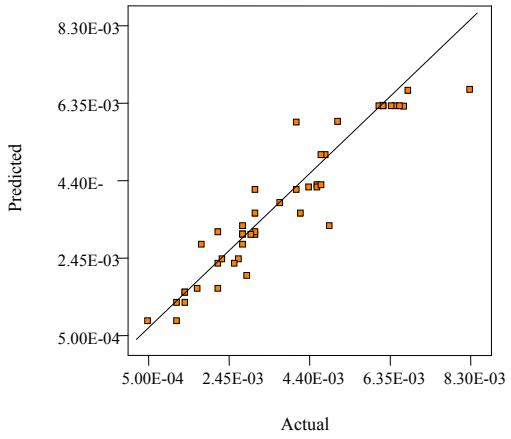


**Figure 16** Predicted versus actual value plot for mass transfer of $CO_2$

Responses from experimental results shown in Figure 16 were well-fitted in acceptable variance range compared to predicted values from the respective empirical model. This indicated that discrepancy occurred due to uncontrollable experimental error could be neglected. Thus, regression model obtained from CCD could be further use a predictor for the optimization of $CO_2$ mass transfer using MGA system.

## 3.5 *Optimization analysis*

In this section, the ultimate goal was to get $CO_2$ mass transfer with moderate DEA concentration and DEA temperature while maintaining others operating conditions. Figure 17, the surface response plot clearly shows that the desirable DEA tends to shift to lower concentration and moderate temperature, around $50^oC$.

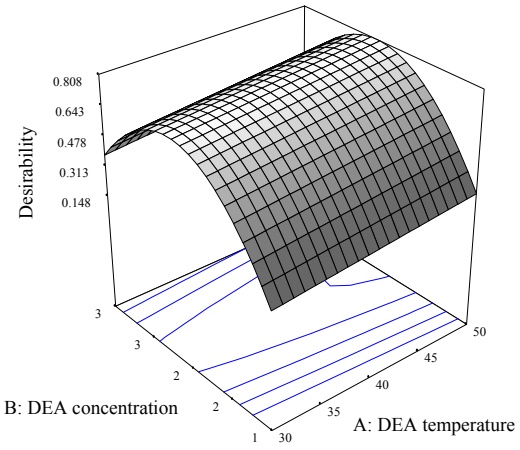


**Figure 17** Response surface plot of desirability

From Table 10, it can be seen that the most desirable operating conditions were set at DEA temperature of 50$^{o}$C, DEA concentration of 2M, DEA velocity of 3770 m/s and DEA flow rate of 80 ml/min, respectively. Meanwhile, for operating condition has no effect to the response; gas flow rate and $CO_2$ inlet concentration were set at 101 ml/min and 33 %v, respectively.

To validate the optimal point generated by CCD, an experimental run was conducted at operating conditions were set as the most desirable operating conditions as shown in Table 10. In the Table 11, the experimental value ($7.97x10^{-3}$ mol/m$^2$s) was found to be in good agreement with the values predicted by CCD ($7.47x10^{-3}$ mol/m$^2$s). Error estimations between predicted and actual values fell within 5%. This indicates that the process optimization in CCD is good and reliable to achieve high $CO_2$ mass transfer when the MGA system is operated using the suggeted optimal operating conditions.

**Table 10** Numerical optimization for central composite design

| **Operating conditions** | **1** | **2** | **3** | **4** | **5** |
|---|---|---|---|---|---|
| DEA temperature ($^{o}$C) | 50 | 50 | 49 | 48 | 48 |
| DEA concentration (M) | 2 | 2 | 2 | 2 | 2 |
| DEA velocity (cm/min) | 3770 | 3770 | 3763 | 3763 | 3763 |
| Gas flow rate (ml/min)* | 101 | 110 | 72 | 70 | 103 |

| | | | | | |
|---|---|---|---|---|---|
| DEA flow rate (ml/min) | 80 | 80 | 79 | 79 | 78 |
| $CO_2$ inlet concentration (%v)* | 33 | 71 | 15 | 62 | 94 |
| Predicted Responses | | | | | |
| Mass transfer of $CO_2$ (mol/($m^2$s)) | $7.47x10^{-3}$ | $7.47x10^{-3}$ | $7.46x10^{-3}$ | $7.45x10^{-3}$ | $7.45x10^{-3}$ |
| Desirability ($D_f$) | 0.90 (Selected) | 0.90 | 0.89 | 0.89 | 0.88 |

*Has no effect on optimization results.

**Table 11** Confirmation between optimized mass transfers of $CO_2$ calculated from mathematical design and experimental study

| **Factor A: DEA temp. ($^oC$)** | **Factor B: DEA con. (M)** | **Factor C: DEA velocity (cm/min)** | **Factor D: Gas flow rate (ml/min)*** | **Factor E: DEA flow rate (ml/min)** | **Factor F: $CO_2$ inlet con. (%v)*** | **Response : Mass Transfer of $CO_2$ (mol/($m^2$s))** |
|---|---|---|---|---|---|---|
| Predicted values from central composite design: | | | | | | |
| 50 | 2 | 3370 | 101 | 80 | 33 | $7.47x10^{-3}$ |
| Actual value from confirmation study: | | | | | | |
| 50 | 2 | 3370 | 101 | 80 | 33 | $7.97x10^{-3}$ |
| Standard deviation (%): | | | | | | 0.04 |

## Conclusions

ANOVA result showed that the temperature, concentration, velocity and flow rate of DEA played a significant role. The optimum DEA temperature was found at 50$^o$C, DEA concentration at 2M, velocity at 3770m/s and 80 ml/min of DEA flow rate with 0.90 of desirability. In the study, the optimum response predicted via CCD was 7.47 x $10^{-3}$ mol/$m^2$s shown good agreement with the actual experiment value 7.97 x $10^{-3}$ mol/$m^2$s with the deviation within 5% between actual and predicted data.

## References

[1] P. Feron, A.Jasen, R. Klaassen, Membrane technology in carbon dioxide removal, Ener. Conver. Manage. 33(1992) 421-428.

[2] S.H. Yeon, K.S. Lee, B. Sea, Y.I. Park, K.H. Lee, Application of pilot-scale membrane contractor hybrid system for removal of carbon dioxide from flue gas, J. Membr. Sci. 257 (2005) 156-160.
[3] R. Wang, Polymeric Membrane preparation and surface modification for water treatment, the 7th International Pre Conference Workshop on Membrane Science & Technology, Kuala Lumpur, (2009).
[4] J.L. Li, B. H. Chen, Review of $CO_2$ absorption using chemical solvents in hollow fiber membrane contactors, Sep. Purif. Technol 41(2005) 109–122.
[5] N. Matsumiya, M. Teramoto, S. Kitada, H. Matsuyama, Evaluation of energy consumption for separation of $CO_2$ in flue gas by hollow fiber facilitated transport membrane module with permeation of amine solution, Sep. Purif. Technol 46 (2005) 33-40.
[6] H. Kreulen,C.A. Smolders, G.F. Versteeg, W.P.M. van Swaaij, Microporous hollow fiber membrane modules as gas-liquid contactors. Part 1. Physical mass transfer processes, J. Membr. Sci. 78 (1993) 197-216.

[7] H. Kreulen,C.A. Smolders, G.F. Versteeg, W.P.M. van Swaaij, Microporous hollow fiber membrane modules as gas-liquid contactors. Part 2. Mass transfer with chemical reaction, J. Membr. Sci. 78 (1993) 217- 238.
[8] H.A. Rangwala, Absorption of Carbon Dioxide into aqueous solutions using hollow fiber membrane contactors, J. Membr. Sci. 112 (1996) 229-240.
[9] R. Wang, D.F. Li, C. Zhou, M. Liu, D.T. Liang, Impact of DEA solutions with and without $CO_2$ loading on porous polypropylene membranes intended for use as contactors, J. Membr. Sci. 229 (2004) 147–157.
[10] F.O. Pedersen, H. Dannstrom, Separation of carbon dioxide from offshore gas turbine exhaust, Ener. Convers. Manage. 38 (1997) 81-86.
[11] N. Nishikawa, M. Ishibashi, H. Ohta,N. Akutsu, H. Matsumoto,T. Kamata, H. Kitamura, $CO_2$ removal by hollow-fiber gas-liquid contactor, Ener. Convers. Manage 36 (1995) 415–418.
[12] S.R. Wickramasinghe, M.J. Semmens, E.L. Cussler, Hollow fiber modules made with hollow fiber fabric, J. Membr. Sci. 84 (1993) 1–14.
[13] K.L. Wang, E.L. Cussler, Baffled membrane modules made with hollow fiber fabric, J. Membr. Sci. 85 (1993) 265–278.
[14] J.G. Lu, Y.F. Zheng, M.D. Cheng, Wetting mechanism in mass transfer process of hydrophobic membrane gas absorption, J. Membr. Sci. 308 (2008) 180–190.
[15] R.J. Little, G.F. Versteeg, W.P.M. van Swaaij, Kinetics of $CO_2$ with primary and secondary amines in aqueous solutions I. Zwitterion deprotonation kinetics for DEA and DIPA in aqueous blends of alkanolamines, Chem. Eng. Sci. 47 (1992) 2027-2035.
[16] D.C. Montgomery, Design and Analysis of Experiments. John Wiley & Sons, New York (2005).
[17] K.M. Lee, D.F. Gillmore, Formulation and process modeling of biopolymer (polyhydroxyalkanoates: PHAs) production from industrial wastes by novel crossed experimental design, Process Biochemistry 40 (2005) 229-246.